Effect of screens on sloshing in a rectangular tank

Odd Faltinsen[1], Alexander Timokha
Dept. Marine Technology & Centre for Ships and Ocean Structures,
Norwegian University of Science and Technology,
NO-7491, Trondheim, Norway; odd.faltinsen@ntnu.no

Screens are used to damp sloshing in antirolling tanks and Tuned Liquid Dampers. An important consideration is that the screen should not significantly affect the highest sloshing period. The damping effect of the screen may for solidity ratios $Sn <\approx 0.5$ be estimated by considering each wire individually, using empirical drag coefficients and by accounting for the blockage effect on the in-flow velocity. The *solidity ratio Sn* is the ratio of the area of the shadow projected by wire meshes on a plane parallel to the screen to the total area contained within the frame of the screen. The Reynolds number based on the wire diameter is small, e.g. 50 in model test conditions. Fig. 1 shows satisfactory agreement between model tests and our linear potential flow theory with nonlinear damping coefficients. The forced longitudinal motion and the longitudinal hydrodynamic force are defined as $\eta_{1a}\sin\sigma t$ and $F_{1a}\sin(\sigma t-\varepsilon_1)$, respectively.

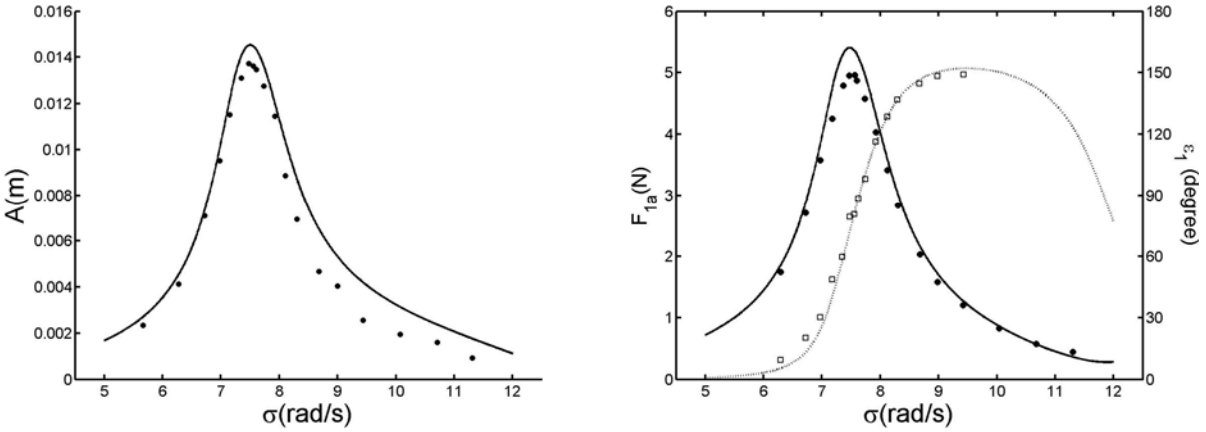

Fig. 1 Steady-state wave amplitude A, longitudinal hydrodynamic force amplitude F_{1a} and phase ε_1 of a rectangular tank with wire mesh $(Sn = 0.48)$ in the middle of the tank that is forced longitudinally with amplitude $\eta_{1a} = 0.002m$ and circular frequency σ. The water depth-to-tank length ratio $h/l = 0.3$. The tank breadth B and length l are $0.2m$ and $0.4m$. The experimental values by Warnitchai & Pinkaew (1995) are denoted as ● and □ (Faltinsen et al., 2009).

A different approach has to be followed for screens with larger solidity ratios and for swash bulkheads. If the ratio between the area of the holes and the area of the bulkhead is small, an important effect is the change of the highest un-compartmented natural sloshing period to a lower value where sloshing is less severe. The effect of perforated plates and screens on natural sloshing frequencies can for any Sn-value be evaluated by using formulae representing the pressure loss through a screen. When $U = U(t)$ is the uniform ambient cross-flow velocity, the pressure loss can be presented as follows

$$\left(p^- - p^+\right) = \tfrac{1}{2} K\rho U\,|\,U\,|\,. \qquad (1)$$

Here p^- and p^+ are the pressures at the two opposite sides of the screen and $K \geq 0$ is the loss coefficient, which is a function of the solidity ratio Sn, Reynolds number and the screen structure. Eq. (1) follows from generalising expressions for steady ambient flow (Blevins, 1992; Roach, 1986) and assuming a small influence of the Keulegan-Carpenter number. The pressure loss coefficient changes from 0 when there is no screen or perforated wall ($Sn = 0$) to ∞ when the screen or perforated plate becomes a solid wall ($Sn = 1$). We consider as an example a rectangular tank with length l and liquid depth h, and a wire-mesh screen as shown in Fig. 2 (a). The tank is forced with sway motions $\eta_2(t) = \eta_{2a}\cos(\sigma t)$. This harmonic forcing excites only

[1] Presenting author

'odd' modes in a rectangular tank without screens. When $Sn = 0$ and $Sn = 1$, the forcing causes resonance at

$$\sigma = \sigma_k^{Sn=0} = \sqrt{g\pi(2k-1)/l \tanh\left(\pi(2k-1)h/l\right)}, \qquad k = 1,2,... \tag{2}$$

$$\sigma = \sigma_k^{Sn=1} = \sqrt{2g\pi(2k-1)/l \tanh\left(2\pi(2k-1)h/l\right)}, \qquad k = 1,2,... \tag{3}$$

The lowest natural modes associated with $\sigma_1^{Sn=0}$ and $\sigma_1^{Sn=1}$ have wave profiles as in Fig. 2 (b) and (c), respectively.

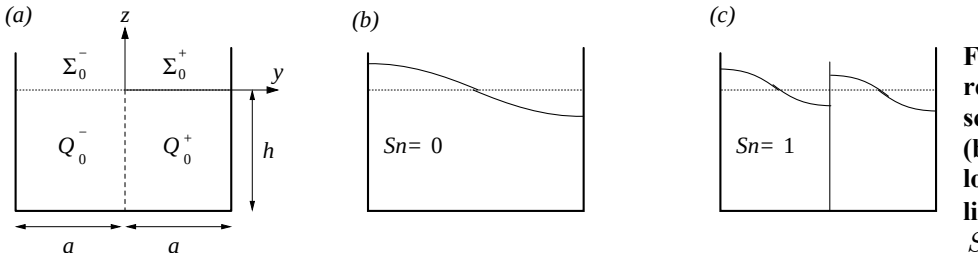

Fig. 2 A two-dimensional rectangular tank with a screen in the middle. Parts (b) and (c) demonstrate the lowest natural modes in the limit cases $Sn = 0$ and $Sn = 1$, respectively.

How the lowest natural frequency changes from $\sigma_1^{Sn=0}$ to $\sigma_1^{Sn=1}$ as Sn varies in the interval $[0,1]$ can be analyzed by using the domain decomposition method with notations in Fig. 2 (a). For each domain Q_0^- and Q_0^+, we introduce the velocity potentials Φ^+ and Φ^-, and the surface waves by $z = \zeta^{\pm}(y,t)$. The boundary conditions of the linear sloshing theory should be fulfilled for $\Phi^{\pm}$ and $\zeta^{\pm}$ on the wall,the bottom and the mean waterplane. In addition, the horizontal velocities on the screen are equal, i.e.

$$U(z,t) = \partial\Phi^+ / \partial y\big|_{y=0} = \partial\Phi^- / \partial y\big|_{y=0}. \tag{4}$$

When assuming that U is known, solving linear sloshing problems in Q_0^- and Q_0^+ makes the velocity potential and, therefore, pressure $p^{\pm} = -\rho(\partial\Phi^{\pm}/\partial t + gz)$ to be functions of U. Substituting the pressure into eq. (1) leads to a nonlinear equation with respect to U. This nonlinear equation has an analytical solution when $U(z,t) = \dot{\eta}_2(t) + \dot{\alpha}_0(t)$. It can be considered as a one-term approximation of the following Fourier representation of the transverse velocity at the screen $U(z,t) = \dot{\eta}_2(t) + \dot{\alpha}_0(t) + \sum_{k=1}^{\infty} \dot{\alpha}_k(t)\cos\left(\pi k(z+h)/h\right)$. The one-term approximation represents a spatially averaged cross-flow along the screen. Our focus is on *steady-state flows due to harmonic forcing*, i.e. $\alpha_0(t) = a_{01}\cos(\sigma t) + a_{02}\sin(\sigma t)$.

An analytical solution of the linear sloshing problem in the domains Q_0^- and Q_0^+ can be found by using the linear modal technique developed for sloshing due to wall deformations (Faltinsen *et al*., 2009). This implies

$$\zeta^{\pm}(y,t) = \pm\alpha_0(t)\ h/a + \sum_{j=1}^{\infty} \beta_j^{\pm}(t)\cos\left(\pi j y/a\right) \tag{5}$$

and an associated modal representation of the velocity potential $\Phi^{\pm}(y,z,t)$ depending on $\alpha_0(t)$ and $\beta_j^{\pm}(t)$. For steady-state solutions, $\beta_j^{\pm}(t) = b_{1j}^{\pm}\cos(\sigma t) + b_{2j}^{\pm}\sin(\sigma t)$ and we can find $b_{1j}^{\pm}$ and $b_{2j}^{\pm}$ analytically as functions of η_{2a} and a_{01}, a_{02}. The harmonically oscillating pressures p^+ and p^- also depend on η_{2a} and a_{01}, a_{02}. Gathering $\cos(\sigma t)$ and $\sin(\sigma t)$-terms in eq. (1) gives the following nonlinear system with respect to a_{01} and a_{02}

$$\eta_{2a}C + a_{01}C_1 = K\frac{h}{\pi\sigma}\int_0^{2\pi/\sigma}\cos(\sigma t)U(t)\,|\,U(t)\,|\,dt = \Lambda a_{02}\sqrt{a_{01}^2 + a_{02}^2},$$

$$a_{02}C_1 = K\frac{h}{\pi\sigma}\int_0^{2\pi/\sigma}\sin(\sigma t)U(t)\,|\,U(t)\,|\,dt = -\Lambda a_{01}\sqrt{a_{01}^2 + a_{02}^2}; \quad \Lambda = K\frac{8h}{3\pi} \tag{6}$$

$$U(t) = \sigma\left[-a_{01}\sin(\sigma t) + a_{02}\cos(\sigma t)\right] = -\sigma\sqrt{a_{01}^2 + a_{02}^2}\,\sin\left(\sigma t - \varepsilon_1\right) = -\rho_0\sigma\sin\left(\sigma t - \varepsilon_1\right),$$

where

$$C = ah + \frac{4a^2}{\pi^3}\sum_{k=1}^{\infty}\frac{(1+(-1)^{k+1})\tanh(\pi kh/a)}{k^3\left(\left(\sigma_k^{Sn=1}\right)^2/\sigma^2 - 1\right)};\;\; C_1 = \frac{2h}{3}\left(a + \frac{h^2}{a}\right) + \frac{4a^2}{\pi^3}\sum_{k=1}^{\infty}\frac{\tanh(\pi kh/a)}{k^3\left(\left(\sigma_k^{Sn=1}\right)^2/\sigma^2 - 1\right)} - \frac{2gh^2}{a\sigma^2}.$$

The solution of the system (6) can be presented as

$$a_{01} = -\eta_{2a}CC_1/\Lambda_1, \qquad a_{02} = \eta_{2a}CC_1\rho_0/\Lambda_1; \qquad \Lambda_1 = C_1^2 + \rho_0^2\Lambda^2, \tag{7}$$

where ρ_0 is a positive root of the nonlinear equation $\eta_{2a}^2C^2 = \rho_0^2\left(C_1^2 + \rho_0^2\Lambda^2\right)$.

For the screens with round wires the loss coefficient can be approximated as (Blevins, 1992; Roach, 1986)

$$K = \beta(1-(1-Sn)^2)/(1-Sn)^2. \tag{8}$$

Here β is a function of the Reynolds number $Rn = U_a d/\nu$ where d is the wire diameter and U_a is the amplitude of the velocity U. The Reynolds number is small for the following studied cases and, generally speaking, causes a variation of β. Based on Blevins (1992), we assume β to be constant. The corresponding table in Blevins (1992) gives $\beta \approx 1.3$ for $Rn = 20$; this is the lowest Rn-value in the table. It is adopted in the forthcoming calculations.

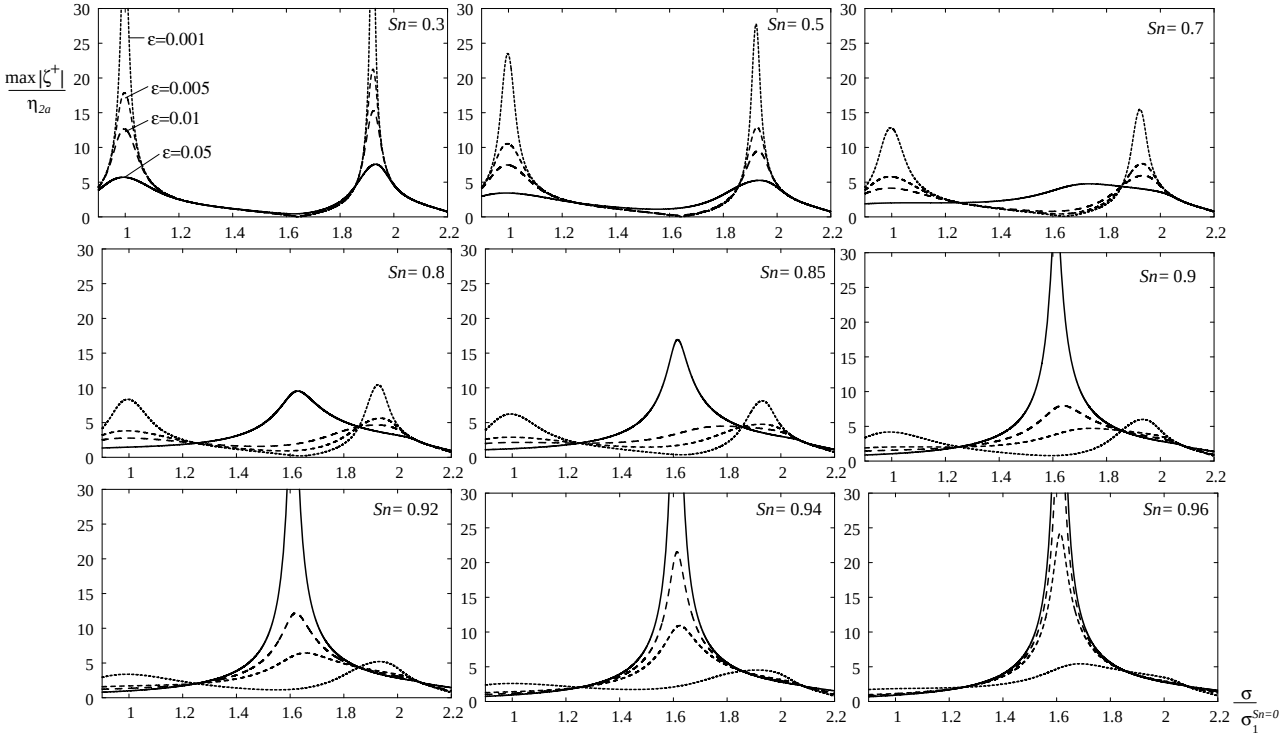

Fig. 3 Maximum non-dimensional wave elevation at the wall versus the forcing frequency for $h/l = 0.3$ and different solidity ratios.

Using the explicit form (8) in eq. (6), we can get an estimate of the resonance frequencies. The first series of numerical examples are presented in Fig. 3 for the maximum wave elevation at the wall, $\max|\zeta^+(a,t)|$ computed by formula (5). It includes resonance response (scaled by the forcing amplitude) for $h/l = h/(2a) = 0.3$ and different solidity ratios. When the solidity ratio is far from 1, e.g. $Sn = 0.3$, Fig. 3 clearly demonstrates resonances at $\sigma = \sigma_1^{Sn=0}$ and $\sigma = \sigma_3^{Sn=0}$ associated with antisymmetric modes in a tank without screens. The larger

nondimensional forcing amplitude η_{2a}/l gives larger damping, i.e. the peaks in Fig. 3 become smaller. When Sn increases, the peaks disappear. However, we see an emerging peak between them corresponding to $\sigma = \sigma_1^{Sn=1}$. This occurs earlier for larger forcing. When $Sn \geq 0.85$ for the presented results, the largest non-dimensional response occurs for the largest forcing, i.e. there is a decreasing flow through the screen with increasing forcing. This tendency is opposite of what happens at lower solidity ratios. If we want to get rid of resonance oscillations in the tank at its lowest natural frequency without a screen, the results imply that the solidity ratio should not be too close to 1 in order to minimize sloshing.

The described method makes it also possible to establish the lowest sloshing frequency versus the solidity ratio. As it is attributed by an equivalent linear mechanical system, the lowest frequency is related to the 90^0 phasing between the input cos-like signal and the surface response. Note, that for studied case, it is the same as the lowest root of the equation $a_{01} = 0 \quad \Leftrightarrow \quad \eta_{2a} D + D_1 = 0$.

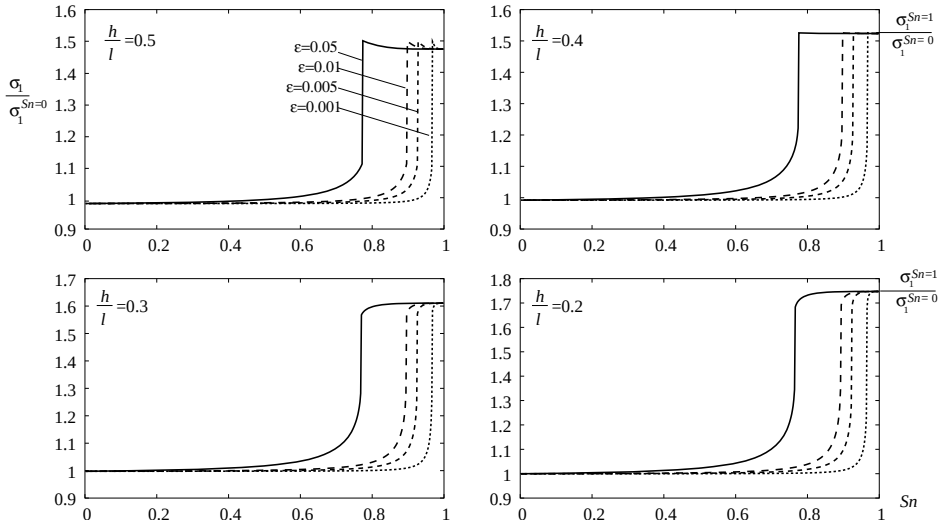

Fig. 4 The lowest natural frequency versus the solidity ratio and different liquid depths and forcing amplitudes.

Results for the lowest sloshing frequency are presented in Fig. 4. Because of the simplification in the approximation of $U = U(t)$, the method gives a small error of $\sigma_1^{Sn=0}$ as $Sn \to 0$. The reason is that the horizontal velocity at $y = 0$ should decay exponentially with submergence. Numerical experiments show that the assumption for U leads to only 0.1% of error for the lowest natural frequency as $h/l \leq 0.5$. The error increases with liquid depth (up to 1% for fairly deep water). It is also larger, up to 5-7% for higher modes, for which exponential decay of the velocity is more important than for the lowest mode. The results do not confirm Dodge's (2000) rule-of thumb that if the total area of the perforations exceed 10% of the bulkhead area, the liquid tends to slosh between the compartments and the slosh natural frequency tends to approach the value of an un-compartmented tank. A reason may be that part of the results in Fig. 4 is for higher forcing amplitudes than Dodge (2000) based his conclusions on. For instance, if the total area of the opening in the screen is less than $\sim 20\%$ of the cross-sectional area of the tank and the ratio ε between the forced sway amplitude and the tank breadth is equal to 0.05, Fig. 4 shows that the lowest un-compartmented natural frequency disappears. The highest sway amplitude divided by the cylinder diameter in the experiments that Dodge referred to was 0.00833. Further, it must be investigated to what extent the fact that Dodge (2000) referred to tests with perforated plates in a vertical circular tank influence the results.

Blevins, R.D. (1992) *Applied Fluid Dynamics Handbook*. Krieger Publishing Company, Florida.

Dodge, F.D. (2000) *The new "Dynamics Behavior of Liquids in Moving Containers"*. Southwest Research Institute, San Antonio, Texas.

Faltinsen, O.M., Rognebakke, O.F., Timokha, A.N. (2009) *Sloshing*. Cambridge University Press.

Roach, P.E. (1987) The generation of nearly isotropic turbulence by means of grids. *J. of Heat and Fluid Flow*, **8**, No. 2, 82-92.

Warnitchai, P., Pinkaew, T. (1998) Modelling of liquid sloshing with flow-dampening devices. *Engineering Structures*, **20**, No. 7, 593-600.